Applied Catalysis B: Environmental 198 (2016) 9–15

Contents lists available at ScienceDirect

Applied Catalysis B: Environmental

journal homepage: www.elsevier.com/locate/apcatb

Oxidative power of aqueous non-irradiated TiO_2-H_2O_2 suspensions: Methylene blue degradation and the role of reactive oxygen species

David Wiedmer[a], Einar Sagstuen[b], Ken Welch[c], Håvard J. Haugen[a], Hanna Tiainen[a,*]

[a] Department of Biomaterials, Institute for Clinical Dentistry, University of Oslo, Norway
[b] Department of Physics, University of Oslo, Norway
[c] Department of Engineering Sciences, The Ångström Laboratory, Uppsala University, Sweden

ARTICLE INFO

Article history:
Received 18 March 2016
Received in revised form 13 May 2016
Accepted 18 May 2016
Available online 18 May 2016

Keywords:
TiO_2
H_2O_2
Methylene blue
Reactive oxygen species
EPR

ABSTRACT

In the present study, the degradation of methylene blue in non-irradiated TiO_2-H_2O_2 suspensions was investigated. Five commercially available catalysts were characterized (BET surface area, zeta potential, hydrodynamic diameter) and their oxidative power was assessed by means of the degradation of methylene blue. A subsequent EPR study was made to verify and identify potential oxidative radicals. The results showed that all suspensions could degrade methylene blue significantly stronger compared to hydrogen peroxide alone. A broad variation between the different catalysts in their capability to adsorb dye molecules was found which was essential for decomposition of methylene blue in darkness. The highest degradation rate of all samples was found for Degussa P25 at neutral pH. EPR studies of this sample verified the presence of oxygen centred radicals namely hydroxyl (•OH) and superoxide radicals ($O_2^{-\bullet}$/•OOH). Non-irradiated TiO_2-H_2O_2 systems show great potential not only in dye removal applications but also in the field of disinfection where low concentrations of hydrogen peroxide are required and irradiation may not be feasible.

1. Introduction

Titanium dioxide (TiO_2) is widely used as a catalyst in heterogeneous photocatalysis in applications such as waste water treatment [1], air purification [1] and disinfection [2] due to its photostability, chemical resistance and cost effectiveness [3]. The oxidative power of TiO_2 particles in aqueous suspension originates from the photogeneration of an electron-hole pair when irradiated ($hf > E_g$) and successive redox reactions with O_2/H_2O [4]. The capacity of TiO_2-UV-systems to degrade organic compounds is strongly related to the generation of reactive products or intermediates of these redox reactions, namely hydroxyl radicals (•OH), superoxide radicals ($O_2^{-\bullet}$), hydroperoxyl radicals (•OOH) and hydrogen peroxide (H_2O_2) [4]. The addition of H_2O_2 has been shown to accelerate TiO_2-assisted photodegradation by its intrinsic oxidative power, repression of electron-hole recombination and photocatalytic reduction to form •OH [5].

Current research focuses strongly on catalyst modifications to make oxidation processes accessible for visible light irradiation and thereby overcome the limitations of UV-irradiation [6–8]. However, TiO_2 particles have also shown to possess oxidative power in the absence of any light when interacting with H_2O_2 [9,10]. Hence, the intrinsic oxidative power of H_2O_2 could be enhanced by the addition of TiO_2 particles. The mechanism behind this Fenton-like reaction is still elusive and contrary studies on the topic have been published [11,12]. While the underlying reaction pathway is controversial, there is evidence that the oxidative behaviour is due the generation of reactive oxygen species (ROS) at the catalyst surface [13,14]. This effect has mostly been studied in the context of nanoparticle toxicity [15–17] and only a few studies have investigated the potential of TiO_2-H_2O_2 systems to degrade organic compounds [9,10,18].

The possibility to degrade organic dyes such as methylene blue (MB) in the absence of light would greatly extend the range of applications for TiO_2 based degradation processes. The oxidative power of a vast selection of photocatalysts has been assessed and relevant operating parameters for the photodegradation of dyes have been addressed [19–22]. To our best knowledge, no such study exists for non-irradiated TiO_2-H_2O_2 systems. The aim of this study was to confirm and assess the oxidative power of five different catalysts in non-irradiated TiO_2-H_2O_2 systems. Special focus was placed on the role of pH dependent adsorption of MB onto the catalyst surface and its influence on the degradation efficacy. Furthermore, an EPR spin trapping study was conducted to verify the presence of ROS

* Corresponding author.
E-mail address: hanna.tiainen@odont.uio.no (H. Tiainen).

http://dx.doi.org/10.1016/j.apcatb.2016.05.036
0926-3373/

and contribute to the knowledge about the degradation mechanism of these systems.

2. Materials and methods

2.1. Materials

Five different TiO_2 powders were used in the present study (Table SI 1): Degussa P25 (**P25**; Evonik Degussa GmbH, Hanau Wolfgang, Germany), Kronos 1171 (**Kro**; Kronos International, Leverkusen, Germany), Hombitan Anatase (**Hom**; Sachtleben Chemie, Duisburg, Germany), Sigma Aldrich rutile (**Ald**; Sigma Aldrich, St. Louis Missouri, United States) and Sensient Eurovit (**Eur**; Sensient colours UK, Lynn Kings, United Kingdom). All powders are commercially available and were used as received without further purification.

Laboratory agent MB and H_2O_2 were used and dilutions were prepared using deionised water (Millipore, Billerica, MA, US). HCl and NaOH were used to adjust the pH. NaCl was used as an inert electrolyte for zeta-potential and hydrodynamic size measurements. For EPR studies, 5,5-dimethyl-1-pyrroline *N*-oxide (DMPO) was used as a spin trap without further purification. All chemicals apart from DMPO (Dojindo Molecular Technologies, Inc, Munich, Germany) were purchased from Sigma Aldrich.

2.2. Zeta potential, hydrodynamic diameter and BET surface area

For zeta potential and hydrodynamic diameter measurements, 50 mg of TiO_2 was added to 1 L 0.001 M NaCl and bath sonicated for 10 min to break up agglomerates. After a resting time of 20 min to allow aggregates to sediment, 300 ml of the supernatant was taken and divided in three stock solutions. Each stock solution was adjusted to pH 3, 6.7 and 9 using HCl and NaOH and stirred for 4 h for pH stabilisation. 1 mL of the sample was then introduced to a disposable folded cuvette (DTS1070, Malvern Instruments, Worcestershire, United Kingdom) and characterized with a Malvern Nano ZS Zetasizer (Malvern Instruments, Worcestershire, United Kingdom). Electrophoretic light scattering (ELS) was utilized to measure the zeta potential using the Smoluchowski equation. Dynamic light scattering (DLS) was used to determine the hydrodynamic diameter calculated derived from the Stokes-Einstein equation. Three measurements were performed for each sample and the same sample was used to measure zeta potential and hydrodynamic diameter.

The specific surface area (SSA) was determined by the adsorption of N_2 at −196 °C using a Micromeritics ASAP 2020 (Norcross, GA, USA). Prior to measurement, all samples were degassed for 12 h at 90 °C. The SSA was calculated using the multipoint BrunauerEmmettTeller (BET) method for adsorption values in the relative pressure range between 0.05 and 0.40.

2.3. Methylene blue adsorption and degradation

The oxidative power of all five TiO_2 powders were tested as followed: 50 mg TiO_2 (C_f = 1 g/L) was added to 47 mL 0.03 mM MB (stirred at 650 rpm) and the pH was adjusted with HCl or NaOH to pH 3, 6.7 or 9. The beaker was covered by an aluminium hood which was only removed quickly for the introduction of titrants or sample extraction to keep the exposure to ambient light at minimum. The suspension was stirred for 60 min to reach the adsorption equilibrium of MB on the TiO_2 particles. For UV–vis measurements of MB absorption, 2 mL samples were taken at 0 (no TiO_2-particles), 5, 10, 15, 30 and 60 min and centrifuged at 10 000 rpm for 1 min. 1.5 mL of the supernatant was then put in a disposable cuvette and analysed using a UVvis spectrophotometer (Lambda 25, PerkinElmer, instruments, MA, USA). The absorbance was recorded for a wavelength range of 750 nm–500 nm and the sample was returned to the stock solution. A pre-study confirmed a maximum absorbance peak at 664 nm with no peak shift in the spectra during the degradation process. A Beer-Lambert diagram was established to correlate the maximum absorbance at 664 nm with different MB concentrations (0.005 mM–0.03 mM). Linear correlation (R^2 = 0.994) was found between absorbance and dye concentration within this range of concentrations.

After one hour of MB absorption, 3 mL of 50 vol.% H_2O_2 was introduced to the suspension to obtain a final concentration of C_f = 3 vol.% H_2O_2. Changes in pH caused by the introduction of H_2O_2 were adjusted with HCl or NaOH. For determination of MB degradation, samples were taken and measured according to the procedure described above at 0, 5, 10, 15, 30 and 60 min. All powders were tested in triplicates for each pH.

2.4. Electron paramagnetic resonance spectroscopy (EPR)

All EPR experiments were carried out under minimum ambient light. 20 mg TiO_2 was mixed with 10 ml 6% H_2O_2 for 30 s. 200 μL of this suspension was taken and introduced to 400 mM DMPO of the same volume. After handshaking for 5 s a sample of approximately 0.05 mL was introduced to a 1.7 mm OD capillary (WILMAD, Vineland, NJ, USA), sealed and inserted into a 707-SQ-250 quartz tube with 4 mm outer diameter (WILMAD, Vineland, NJ, USA). The sample was then placed in a universal rectangular TE_{102} cavity and EPR measurements were started immediately using a BRUKER EleXsyS 560 X-band spectrometer (Rheinstetten, Germany). All measurements were performed at a microwave frequency of 9771 MHz and microwave power of 12.6 mW. Measurements were done at a centre field of 348.2 mT, a sweep field of 8 mT and a field scan rate of 0.048 mT/s. The field modulation frequency was set to 100 kHz with a modulation width of 0.08 mT. A time constant of 167 ms was used. A first harmonic order spectrum was recorded for each sample approx. 90 s after the introduction of the spin trap.

2.5. Statistics

Datasets were analysed using a normality and equal variance test prior to further statistical testing. One-way analysis of variance (ANOVA) and a subsequent pairwise comparison of data groups (TiO_2 + H_2O_2) versus a control group (H_2O_2 only) using Holm-Sidak method was done to determine statistical significance in dye degradation, zeta potential and hydrodynamic size. Probability of $p < 0.05$ was considered significant with n = 3 samples for each group. All statistical analyses were performed using SigmaPlot 13.0 (Systat Software Inc., Chicago, IL).

3. Results & discussion

3.1. Zeta potential, hydrodynamic diameter and BET surface area

The adsorption of dye molecules onto the catalyst surface may play an essential role in the irradiation independent degradation of MB. Therefore, all tested TiO_2 powders were characterized regarding surface charge (zeta potential) and potentially available adsorption sites (BET surface area and hydrodynamic diameter). Table 1 presents the zeta potential, hydrodynamic diameter and BET surface area of the five TiO_2 powders tested. An increase in pH resulted in more negative zeta potentials for all tested TiO_2 powders and the absolute values measured are consistent with previous results [23–25]. Interestingly, zeta potentials close to the isoelectric point (iep) were observed for Kro and Eur at pH 3. This was different from the other TiO_2 samples for which positive zeta potentials were

Table 1
Adsorption related properties of five TiO_2 powders (mean ± SD, n = 3).

Sample‘	BET (m^2/g)	Zeta potential (mV)			Hydrodynamic diameter (nm)		
		pH 3	pH 6.7	pH 9	pH 3	pH 6.7	pH 9
P25	53.6 ± 0.6	28.1 ± 0.4	−13.9 ± 0.7	−36.6 ± 0.1	526 ± 18	3648 ± 137	2240 ± 199
Kro	6.1 ± 0.1	1.5 ± 0.6	−46.8 ± 1.3	−50.7 ± 1.6	1743 ± 77	281 ± 12	342 ± 37
Eur	7.7 ± 0.1	−5.4 ± 0.6	−46.4 ± 1.2	−50.6 ± 0.9	1540 ± 301	368 ± 14	401 ± 32
Hom	11.2 ± 0.2	11.1 ± 0.2	−36.2 ± 0.2	−45.9 ± 0.3	1257 ± 423	1850 ± 194	1341 ± 107
Sig	4.2 ± 0.1	16.7 ± 0.5	−18.8 ± 5.4	−29.2 ± 1.3	1806 ± 630	1447 ± 205	861 ± 342

measured at this pH. This indicated a shift of the iep towards more acidic environments for Kro and Eur compared to pure anatase TiO_2 which may be caused by impurities, such as phosphates, originating from the fabrication process and was has previously been reported previously for Kro [26,27]. A negatively charged catalyst surface over a wide range of pH is generally favourable for dye degradation due to higher electrostatic attraction between the dye and the catalyst. However, the presence of impurities may also decrease the degradation efficacy [28].

The BET surface areas of the tested TiO_2 particles were comparable to each other with one exception: P25 had an approx. 10 fold larger surface area compared to the other tested TiO_2 powders and thereby intrinsically possesses higher adsorptive capacity (Table 1). In addition to BET measurements the hydrodynamic diameter was measured as an indicator for potential adsorption sites in colloidal suspension. An increase in diameter was found for all tested samples at pH close to their iep (Table 1). This can be explained by the formation of agglomerates due to the reduction of repulsive forces and dominance of attractive van der Waals forces as described in the DLVO theory [29,30]. These agglomerates reduce the surface area available for dye adsorption and may therefore also decrease the degradation efficiency [31]. A different behaviour is possible for agglomerates which consist of nano-scale primary particles (P25) which may retain high surface area for adsorption even when agglomerated. Further, the hydrodynamic diameter differed strongly from primary particle sizes specified by the producers even at pH of high zeta potentials (>±30 mV). This may be due to aggregates which could not be broken up during bath sonication and potentially further reduce adsorption capacities of the TiO_2 powders.

4. Methylene blue degradation

4.1. Adsorption

The pH dependent MB adsorption on TiO_2 powders is shown in Fig. 1A. The equilibrium concentration of MB after 60 min adsorption onto the surface of different TiO_2 particles at pH 3, 6.7 and 9 was calculated as followed:

$$q_e = \frac{(C_0 - C_e)\,MV}{m}$$

where q_e (mg_{MB}/g_{TiO2}) is the equilibrium adsorption of MB on TiO_2, C_0 ($mol\,L^{-1}$) is the initial MB concentration, C_e ($mol\,L^{-1}$) is the equilibrium MB concentration, M ($g\,mol^{-1}$) is the molar mass of MB, V (L) is the volume of the solution and m (g) is the mass of the catalyst.

An increase in solution pH resulted in an increased dye adsorption for all samples (Fig. 1A). This correlates with the surface charge of TiO_2 at pH > iep at which the surface becomes negatively charged due to the predominance of TiO^- surface groups which favour the adsorption of cationic MB. This explains the statistically significant adsorption for Kro and Eur at neutral and alkaline conditions ($p_{kro} = p_{eur} < 0.001$) and P25 at pH 9 ($p < 0.001$). The strongest adsorption capacity of all tested TiO_2 powders was observed for P25 at this pH and could be attributed to the large surface area and a strong negative surface charge (Table 1). However, surface charge alone was not sufficient to explain q_e at different pH for all tested TiO_2 powders. Sig and Hom showed only minor adsorption even in alkaline suspensions. One explanation was that both powders have low available adsorption sites compared to the other powders. The BET surface area for Sig was comparably low and the hydrodynamic diameter of Hom remained high even in suspension of high zeta potential values where strong repulsive forces between the particles are present (Table 1). It should also be noted that the absolute value for q_e in this study did not derive from an adsorption isotherm study but is rather used as a measure to compare the adsorption capacity of different catalysts at one initial dye concentration.

4.2. Degradation

After 1 h adsorption time in darkness, H_2O_2 was introduced to start the irradiation independent degradation of MB. Fig. 1B–D displays the normalised degradation curves for MB in non-irradiated TiO_2-H_2O_2 suspensions at the different pH levels. It should be noted that the introduction of H_2O_2 influenced the measured absorbance in various other ways (dilution, adsorption/desorption processes, see supplementary information) than through the interaction of H_2O_2 and TiO_2.

The strongest degradation for all five tested TiO_2 powders was observed at pH 6.7 (Fig. 1C). Among all TiO_2-H_2O_2 suspensions at this pH, the strongest degradation was found for P25 suspensions, which were capable of degrading MB completely within 10 min after the introduction of H_2O_2. Interestingly, no statistically significant adsorption was observed for P25 at this pH after the equilibrium phase. However, a distinct change in the colour of the suspension was visible shortly after the introduction of H_2O_2 and the re-adjustment to pH 6.7. While the colour of the suspension was pale blue before the introduction of H_2O_2 it turned purple afterwards (Fig. 2A–B). Purple suspensions were also observed in experiments using TiO_2 catalysts with high q_e (Kro, Eur), and this appearance has been attributed to the adsorption of oxidized form of MB ($MB^{\bullet+}$) onto the surface of the catalyst [32]. These observations suggest that the introduction of H_2O_2 favours the adsorption of MB. One possible explanation for this is a change in surface potential of the catalyst caused by the adsorption of superoxide radical anions as described later in this article. No purple colour was observed after 60 min of degradation for the suspension or TiO_2 particles derived from the suspension (Fig. 2C1–C2). The yellowish appearance of the particles is likely to be caused by the formation of a peroxy titanate complex at the catalyst surface which has been previously described for P25 [10]. The absence of blue or purple colour in both suspension and particles indicates that no adsorbed MB is present and that the disappearance of MB for P25-H_2O_2 at pH 6.7 is due to complete degradation of MB.

The superior degradation of P25 compared to the other tested TiO_2 samples is likely a consequence of low primary particle size and the high surface area. For powders of similar BET surface area (Kro, Eur, Sig and Hom), a strong dependency between equilibrium adsorption and dye degradation was found: groups with high q_e (Kro, Eur) showed stronger degradation compared to groups with

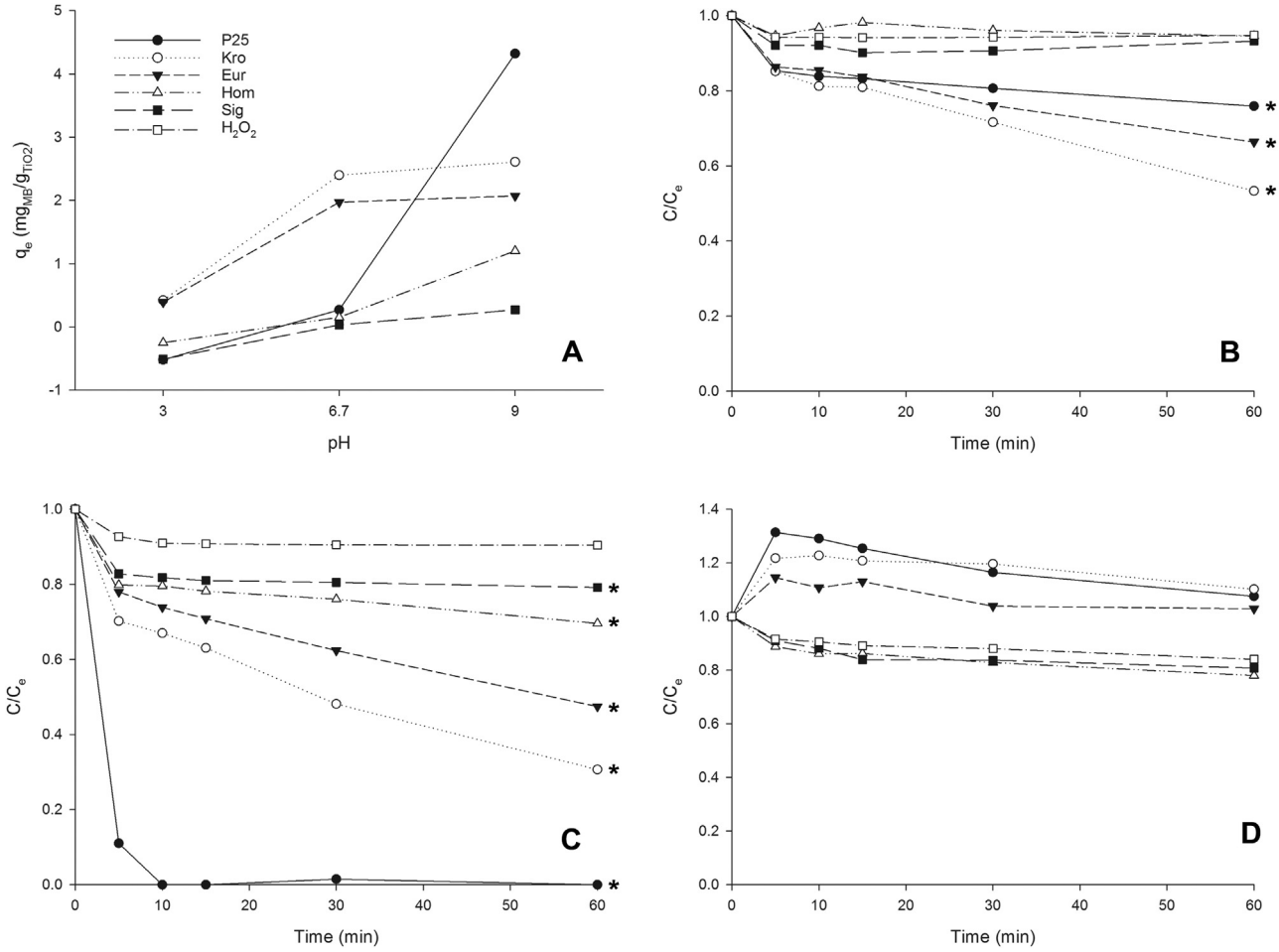

Fig. 1. (A) pH dependent MB adsorption on TiO_2 powders and normalised degradation curves for MB in non-irradiated TiO_2-H_2O_2 suspensions at (B) pH 3, (C) pH 6.7 and (D) pH 9 in darkness (mean). * Statistically significant difference in MB degradation after 60 min between TiO_2-H_2O_2 suspensions and H_2O_2 alone ($p < 0.05$, $n = 3$).

low q_e (Sig, Hom) at pH 3 and pH 6.7 (Fig. 1B–C). On the other hand, the degradation behaviour in alkaline suspensions was different compared to that at pH 3 and pH 6.7 (Fig. 1D). An increase in q_e did not result in an increase in MB degradation at pH 9. The most likely reason for this was the strong desorption process observed after the introduction of H_2O_2 due to a decrease in pH (Fig. 1D, see supplementary information). Dye adsorption onto the catalyst surface is likely to be the rate determining factor, and therefore, re-adsorption may lower the measured degradation. This illustrates the diverse role of solution pH not only in TiO_2 photodegradation [33] but also in non-irradiated systems.

The results indicate that dye adsorption onto the catalysts surface is needed to achieve degradation in non-irradiated TiO_2-H_2O_2 systems. This relation is also well known for irradiated TiO_2-H_2O_2 systems [34] and may be associated with the generation of radicals at the catalyst surface. However, more surface specific oxidative compounds such as photogenerated holes are present in an irradiated system and a direct comparison between the two systems should be avoided. It should also be noted that even though the exposure time to ambient light was reduced to a minimum, complete darkness could not be assured. Hence, it has to be considered whether dye degradation could possibly originate from the interaction with ambient light. The excitement of an electron into the conduction band of non-doped TiO_2 requires irradiation in the UV-range but electron transfer from a sensitized dye to the TiO_2 conduction band could provoke an oxidative effect at ambient light [35]. However, the degradation capacity of visible light irradiated TiO_2 is significantly lower [36] and is not sufficient to explain the strong degradation detected. Therefore, these findings relate the oxidative effect to the interaction of TiO_2 and H_2O_2 in darkness.

4.3. EPR spin trapping

The results for MB degradation in non-irradiated TiO_2-H_2O_2 suspensions indicate a strong oxidative behaviour at the catalyst surface or in its proximity. An EPR spin trapping study was conducted in order to verify the presence of radicals and identify radical species which may be responsible for the degradation of MB. The spectra for P25, Kro and Eur (Fig. 3) showed two characteristic signals of similar intensity. The observed hyperfine splitting constants (hfsc's) for the 1:2:2:1 signal ($a_N = a_H = 1.48$ mT) are in good accordance with literature values found for the •OH spin adduct of DMPO [37]. The hfcs for the second signal ($a_N = 1.42$ mT, $a_H\beta = 1.12$ mT and $a_H{}^{\gamma} = 0.12$ mT) could be attributed to the DMPO spin adduct of $O_2{}^{-\bullet}$/•OOH [37]. Most interestingly, $O_2{}^{-\bullet}$/•OOH were only present for TiO_2 samples which also showed high degradation rates of MB (P25, Kro and Eur) but not for samples with low degradation rates (Hom and Sig) (Fig. 3, also see supplementary information). Yet, strong •OH signals were observed for Hom and Sig and also for H_2O_2 without TiO_2 particles. A subsequent experiment with ethanol confirmed the presence of •OH for aqueous H_2O_2 solutions (Supplementary information). Hence, •OH in aqueous H_2O_2 solutions may be generated by autolysis or its interaction with DMPO rather than by the interaction with TiO_2. The reduction in signal

Fig. 2. Appearance of P25 suspensions at pH 6.7 during the adsorption and degradation process: (A) shortly before, (B) shortly after and (C1) 60 min after the introduction of H_2O_2. (C2) shows the appearance of P25 particles received from (C1) after filtration.

intensity of DMPO-OH for P25, Kro and Eur is likely to arise from the competitive reaction of $O_2^{-\bullet}$/•OOH and •OH with the spin trap. However, it is also possible that •OH functioned as a precursor in the formation of $O_2^{-\bullet}$/•OOH and thereby less •OH radicals were present in those suspensions.

The generation of ROS at the TiO_2 surfaces when in contact with H_2O_2 is still controversial and only weak signals have been observed in similar studies [12,15,38,39]. The presented data indicate the presence of ROS, namely $O_2^{-\bullet}$/•OOH and •OH, for the interaction of TiO_2 with aqueous H_2O_2 solutions in darkness. This supports earlier EPR studies by Sánchez et al. [9] who also observed both ROS for a similar experimental setup but higher concentrations of both TiO_2 and H_2O_2. Our results further point out the essential role of $O_2^{-\bullet}$/•OOH rather than •OH in the degradation of MB in non-irradiated TiO_2-H_2O_2 suspensions. Only TiO_2-H_2O_2 suspensions for which EPR spectra contained $O_2^{-\bullet}$/•OOH showed high MB degradation rates. Yet, the formation of •OH is energetically more favourable with respect to $O_2^{-\bullet}$/•OOH formation at anatase surfaces [40] and •OH is known to be the most reactive among oxygen centred radicals [41]. However, surface stabilised •OH may also have adverse effect on subsequent reactions [42], and further studies are needed to clarify the role of •OH in TiO_2-H_2O_2 suspensions.

One possible explanation for the dominant role of $O_2^{-\bullet}$/•OOH may be the stabilisation of this radical, particular in the unprotonated $O_2^{-\bullet}$ form, on the TiO_2 surface similar to what has been shown for H_2O_2 treated, dried ZrO_2 [43,44]. Adsorbed radicals may contribute to the observed degradation in two different ways: superoxide radical anions $O_2^{-\bullet}$ which bind to the surface may result in a more negative surface potential and thereby favouring the adsorption of cationic dyes such as MB. This is the most likely reason for the different adsorption behaviour of P25 at pH 6.7 before and after the introduction of H_2O_2 (Fig. 2A–B). Further, adsorbed $O_2^{-\bullet}$/•OOH may contribute to the subsequent degradation of adsorbed MB by creating an oxidative environment at the solid-liquid interface. This is also supported by the strong dependency on prior dye adsorption for the degradation of MB (Fig. 1, Fig. 2). Further studies have to be conducted to elucidate possible reaction pathways and clarify the role of •OH.

5. Conclusion

The present study showed that MB could be decomposed by the interaction of TiO_2 and low concentrated H_2O_2 in darkness. A comparison of five commercially available TiO_2 powders showed a strong dependency of degradation on prior dye adsorption onto the catalyst surface. The adsorption capacity varied strongly between the tested powders and solution pH. The strongest degradation was found for Degussa P25 at neutral pH. In an EPR study, the presence of oxygen centred radicals (•OH and $O_2^{-\bullet}$/•OOH) was verified. MB degradation was found to be dependent on the generation of $O_2^{-\bullet}$/•OOH.

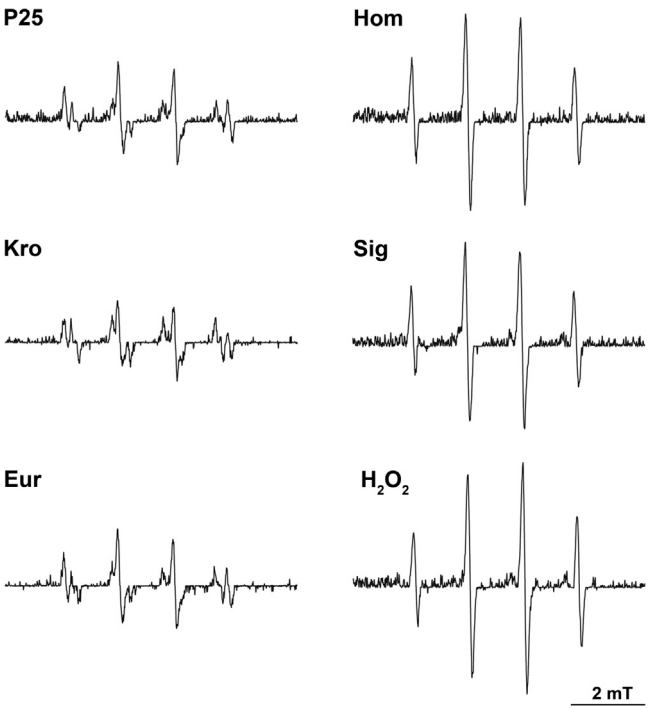

Fig. 3. EPR spectra of H_2O_2 suspensions with different TiO_2 catalysts in darkness. All spectra were recorded approx. 90 s after the introduction of DMPO.

Acknowledgment

This study was supported by EUREKA Eurostars E!8320 NuGel.

Appendix A. Supplementary data

Supplementary data associated with this article can be found, in the online version, at http://dx.doi.org/10.1016/j.apcatb.2016.05.036.

References

[1] A. Mills, R.H. Davies, D. Worsley, Water purification by semiconductor photocatalysis, Chem. Soc. Rev. 22 (1993) 417–425.
[2] H.A. Foster, I.B. Ditta, S. Varghese, A. Steele, Photocatalytic disinfection using titanium dioxide: spectrum and mechanism of antimicrobial activity, Appl. Microbiol. Biotechnol. 90 (2011) 1847–1868.
[3] O. Carp, C.L. Huisman, A. Reller, Photoinduced reactivity of titanium dioxide, Prog. Solid State Chem. 32 (2004) 33–177.
[4] U.I. Gaya, A.H. Abdullah, Heterogeneous photocatalytic degradation of organic contaminants over titanium dioxide: a review of fundamentals, progress and problems, J. Photochem. Photobiol. C: Photochem. Rev. 9 (2008) 1–12.
[5] T. Hirakawa, Y. Nosaka, Properties of O_2-and OH formed in TiO_2 aqueous suspensions by photocatalytic reaction and the influence of H_2O_2 and some ions, Langmuir 18 (2002) 3247–3254.
[6] M. Maeda, T. Watanabe, Visible light photocatalysis of nitrogen-doped titanium oxide films prepared by plasma-enhanced chemical vapor deposition, J. Electrochem. Soc. 153 (2006) C186–C189.
[7] M. Pelaez, N.T. Nolan, S.C. Pillai, M.K. Seery, P. Falaras, A.G. Kontos, P.S.M. Dunlop, J.W.J. Hamilton, J.A. Byrne, K. O'Shea, M.H. Entezari, D.D. Dionysiou, A review on the visible light active titanium dioxide photocatalysts for environmental applications, Appl. Catal. B: Environ. 125 (2012) 331–349.
[8] A.R. Khataee, M.N. Pons, O. Zahraa, Photocatalytic degradation of three azo dyes using immobilized TiO_2 nanoparticles on glass plates activated by UV light irradiation: influence of dye molecular structure, J. Hazard. Mater. 168 (2009) 451–457.
[9] L.D. Sanchez, S.F.M. Taxt-Lamolle, E.O. Hole, A. Krivokapic, E. Sagstuen, H.J. Haugen, TiO_2 suspension exposed to H_2O_2 in ambient light or darkness: degradation of methylene blue and EPR evidence for radical oxygen species, Appl. Catal. B Environ. 142 (2013) 662–667.
[10] C. Randorn, S. Wongnawa, P. Boonsin, Bleaching of methylene blue by hydrated titanium dioxide, ScienceAsia 30 (2004) 149–156.
[11] Y.F. Rao, W. Chu, Reaction mechanism of linuron degradation in TiO_2 suspension under visible light irradiation with the assistance of H_2O_2, Environ. Sci. Technol. 43 (2009) 6183–6189.
[12] X. Li, C. Chen, J. Zhao, Mechanism of photodecomposition of H_2O_2 on TiO_2 surfaces under visible light irradiation, Langmuir 17 (2001) 4118–4122.
[13] C.M. Lousada, A.J. Johansson, T. Brinck, M. Jonsson, Mechanism of H_2O_2 decomposition on transition metal oxide surfaces, J. Phys. Chem. C 116 (2012) 9533–9543.
[14] A. Hiroki, J.A. LaVerne, Decomposition of hydrogen peroxide at water-ceramic oxide interfaces, J. Phys. Chem. B 109 (2005) 3364–3370.
[15] I. Fenoglio, G. Greco, S. Livraghi, B. Fubini, Non-UV-induced radical reactions at the surface of TiO_2 nanoparticles that may trigger toxic responses, Chem. A Eur. J. 15 (2009) 4614–4621.
[16] R.P.F. Schins, A.M. Knaapen, Genotoxicity of poorly soluble particles, Inhal. Toxicol. 19 (2007) 189–198.
[17] B. Fubini, M. Ghiazza, I. Fenoglio, Physico-chemical features of engineered nanoparticles relevant to their toxicity, Nanotoxicology 4 (2010) 347–363.
[18] M. Jose, M.P. Haridas, S. Shukla, Predicting dye-adsorption capacity of hydrogen titanate nanotubes via one-step dye-removal method of novel chemically-activated catalytic process conducted in dark, J. Environ. Chem. Eng. 2 (2014) 1980–1988.
[19] U.G. Akpan, B.H. Hameed, Parameters affecting the photocatalytic degradation of dyes using TiO_2-based photocatalysts: a review, J. Hazard. Mater. 170 (2009) 520–529.
[20] R. Daghrir, P. Drogui, D. Robert, Modified TiO_2 for environmental photocatalytic applications: a review, Ind. Eng. Chem. Res. 52 (2013) 3581–3599.
[21] B. Zielińska, J. Grzechulska, R.J. Kaleńczuk, A.W. Morawski, The pH influence on photocatalytic decomposition of organic dyes over A11 and P25 titanium dioxide, Appl. Catal. B: Environ. 45 (2003) 293–300.
[22] M.L. Fetterolf, H.V. Patel, J.M. Jennings, Adsorption of methylene blue and acid blue 40 on titania from aqueous solution, J. Chem. Eng. Data 48 (2003) 831–835.
[23] J. Jiang, G. Oberdörster, P. Biswas, Characterization of size, surface charge, and agglomeration state of nanoparticle dispersions for toxicological studies, J. Nanopart. Res. 11 (2009) 77–89.
[24] K. Suttiponparnit, J. Jiang, M. Sahu, S. Suvachittanont, T. Charinpanitkul, P. Biswas, Role of surface area, primary particle size, and crystal phase on titanium dioxide nanoparticle dispersion properties, Nanoscale Res. Lett. 6 (2011) 1–8.
[25] M. Kosmulski, The pH-dependent surface charging and points of zero charge: v. Update, J. Colloid Interface Sci. 353 (2011) 1–15.
[26] R. Sabetrasekh, H. Tiainen, J.E. Reseland, J. Will, J.E. Ellingsen, S.P. Lyngstadaas, H.J. Haugen, Impact of trace elements on biocompatibility of titanium scaffolds, Biomed. Mater. 5 (2010) 015003.
[27] H. Tiainen, S.P. Lyngstadaas, J. Ellingsen, H. Haugen, Ultra-porous titanium oxide scaffold with high compressive strength, J. Mater. Sci. 21 (2010) 2783–2792.
[28] C. Guillard, E. Puzenat, H. Lachheb, A. Houas, J.-M. Herrmann, Why inorganic salts decrease the TiO_2 photocatalytic efficiency, Int. J. Photoenergy 7 (2005) 1–9.
[29] B. Derjaguin, Theory of the stability of strongly charged lyophobic sols and the adhesion of strongly charged particles in solutions of electrolytes, Acta Physicochim. USSR 14 (1941) 633–662.
[30] E.J.W. Verwey, J.T.G. Overbeek, J.T.G. Overbeek, Theory of the stability of lyophobic colloids Courier Corporation, (1999).
[31] M.H. Habibi, A. Hassanzadeh, S. Mahdavi, The effect of operational parameters on the photocatalytic degradation of three textile azo dyes in aqueous TiO_2 suspensions, J. Photochem. Photobiol. A: Chem. 172 (2005) 89–96.
[32] C. Randorn, J.T.S. Irvine, P. Robertson, Synthesis of visible-Light-Activated yellow amorphous photocatalyst, Int. J. Photoenergy 2008 (2008) 6.
[33] I.K. Konstantinou, T.A. Albanis, TiO_2-assisted photocatalytic degradation of azo dyes in aqueous solution: kinetic and mechanistic investigations: a review, Appl. Catal. B: Environ. 49 (2004) 1–14.
[34] K. Rajeshwar, M. Osugi, W. Chanmanee, C. Chenthamarakshan, M.V.B. Zanoni, P. Kajitvichyanukul, R. Krishnan-Ayer, Heterogeneous photocatalytic treatment of organic dyes in air and aqueous media, J. Photochem. Photobiol. C: Photochem. Rev. 9 (2008) 171–192.
[35] L. Pan, J.-J. Zou, X. Zhang, L. Wang, Water-mediated promotion of dye sensitization of TiO_2 under visible light, J. Am. Chem. Soc. 133 (2011) 10000–10002.
[36] X.Z. Li, F.B. Li, Study of Au/Au3+-TiO_2 photocatalysts toward visible photooxidation for water and wastewater treatment, Environ. Sci. Technol. 35 (2001) 2381–2387.
[37] G.R. Buettner, Spin trapping: eSR parameters of spin adducts1474 1528 V, Free Radic. Biol. Med. 3 (1987) 259–303.
[38] M.-C. Lee, F. Yoshino, H. Shoji, S. Takahashi, K. Todoki, S. Shimada, K. Kuse-Barouch, Characterization by electron spin resonance spectroscopy of reactive oxygen species generated by titanium dioxide and hydrogen peroxide, J. Dent. Res. 84 (2005) 178–182.
[39] P. Tengvall, I. Lundström, L. Sjöqvist, H. Elwing, L.M. Bjursten, Titanium-hydrogen peroxide interaction: model studies of the influence of the inflammatory response on titanium implants, Biomaterials 10 (1989) 166–175.

[40] W.-F. Huang, P. Raghunath, M.C. Lin, Computational study on the reactions of H_2O_2 on TiO_2 anatase (101) and rutile (110) surfaces, J. Comput. Chem. 32 (2011) 1065–1081.
[41] G.R. Buettner, The pecking order of free radicals and antioxidants: lipid peroxidation, α-tocopherol, and ascorbate, Arch. Biochem. Biophys. 300 (1993) 535–543.
[42] C.M. Lousada, M. Yang, K. Nilsson, M. Jonsson, Catalytic decomposition of hydrogen peroxide on transition metal and lanthanide oxides, J. Mol. Catal. A: Chem. 379 (2013) 178–184.
[43] M. Anpo, M. Che, B. Fubini, E. Garrone, E. Giamello, M. Paganini, Generation of superoxide ions at oxide surfaces, Top. Catal. 8 (1999) 189–198.
[44] E. Giamello, P. Rumori, F. Geobaldo, B. Fubini, M.C. Paganini, The interaction between hydrogen peroxide and metal oxides: EPR investigations, Appl. Magn. Reson. 10 (1996) 173–192.